ISSN 2354-9114 (online), ISSN 0024-9521 (print)
Indonesian Journal of Geography Vol 57, No.1 (2025): 42-51
DOI: 10.22146/ijg.91332 website: https://jurnal.ugm.ac.id/ijg

INDONESIAN JOURNAL OF GEOGRAPHY

RESEARCH ARTICLE

Simeulue Earthquake Activity Analysis Using the MLE Method

Henry Junus Wattimanela[1, 2, *)], Nanang T. Puspito[3], and Harmanus Batkunde[1]
[1]Department of Mathematics, Faculty of Mathematics and Natural Sciences, Pattimura University, Ambon, Maluku, Indonesia.
[2]Geostatistics Laboratory, Faculty of Mathematics and Natural Sciences, , Pattimura University, Ambon, Maluku, Indonesia.
[3]Global Geophysics Research Group, Faculty of Mining and Petroleum Engineering, Institut Teknologi Bandung, Bandung, Jawa Barat, Indonesia

Received: 2023-12-02
Revised: 2024-01-11
Accepted: 2024-12-07
Published: 2025-04-27

Key words: MLE method; return period; seismicity index; Simeulue Regency; tectonic earthquake

Correspondent email :
hwattimanela@gmail.com

Abstract The territory of Indonesia is prone to a high level of tectonic earthquake vulnerability including In Simeulue Regency, one of the regions of Aceh Province. Therefore, this study aimed to analyze level of tectonic earthquake activity in Simeulue Regency and its surroundings divided into four Sub Regions (I, II, III, and IV). The data used spanned 1940-2020 and were sourced from the ISC with the criteria of the depth being <60km and a magnitude of 3Mw. The seismic features were elucidated through descriptive statistics, while the determination of 'a' and 'b' values for individual Sub Region was accomplished by using the maximum likelihood estimation (MLE) method. The results showed that the highest distribution of earthquakes was at a depth of 15-44.9 km and magnitude at intervals of 3.0-4.9 Mw, specifically in Sub Region III. The largest Mc value was found in Sub Region I, while Sub Region III had high seismic activity and rock heterogeneity. In addition, this area had a large seismicity index and the shortest return period at intervals of magnitude $3.0 \leq M < 4.0$. Sub Region I on the other hand had a longer seismicity index at intervals of magnitudes $4.0 \leq M < 5.0, 5.0 \leq M < 6.0$, and $M \geq 6.0$.

1. Introduction

Tectonic earthquake is among the most formidable natural catastrophes, capable of inflicting harm on residential areas and resulting in casualties. This phenomenon also has the potential to set off additional calamities, including the formation of tsunamis. In general, the greater the magnitude and intensity of earthquake, the more severe the damage caused (Nampally et al., 2018; Jafari, 2010; Lines et al., 2022). Indonesia falls within the classification of earthquake-prone region due to its location at the convergence of three significant tectonic plates namely Eurasia, Indo-Australia, and the Pacific (Luschen et al, 2011, & Ramdani et al., 2019). One of earthquake-prone areas is Simeulue Regency, primarily due to the interaction of the subduction zone between the India-Australian and the Eurasian Plate. The significant earthquake of 1907, estimated to have a magnitude ranging from 7.5 to 8.0 Ms struck Aceh, leading to the rupture of the upper and shallower megathrust segments of Nias Southern Simeulue. This incident had devastating consequences, including the destruction of the South Coast of Simeulue, causing the Island to nearly submerge, and the loss of 50-70% of the population. In December 2004, another earthquake with a magnitude of 9.2 occurred, resulting in seven fatalities. The 2005 incidence was associated with an uplift in the Southern Part of Simeulue which peaked at 50 cm extending from the southernmost West Coast of Nias to the North End of the island and the North to the East Simeulue. This earthquake caused a tsunami of 3-4m but no casualties (Meltzner et al, 2015, Rahman et al., 2018).

To mitigate the consequences of earthquake events, it is essential to obtain a prediction or an estimate of return period. This estimation can be acquired by determining the values of two crucial activity parameters namely 'a,' reflecting seismicity of an area, and 'b,' characterizing tectonic conditions (Henderson et al, 1994; Sharma et al, 2013; Gorgun, 2013; El-Nader, 2016; and Gunti et al, 2022). The determination of these two parameters is expected to identify areas that have the potential to cause earthquake in the future for mitigation efforts. Furthermore, the Maximum Likelihood Method (MLE) is a statistical method well-suited for addressing various seismological challenges and offers advantages in the computation of earthquake activity parameter values ('a' and 'b'). This method can be used to statistically calculate the seismic activity parameter values from the Guttenberg-Richter (GR) Law equation, seismicity index, earthquake risk level, and return period.

Several previous studies have applied the MLE method, including Kladivko and Rusy (2022) who examined the Hull-White model implemented on EUR interest rate data. In 2022, Liu used the Maximum Likelihood Estimation (MLE) method to forecast the comprehensive elemental composition of coal, comprising C, H, O, N, and S, achieving a predictive accuracy suitable for engineering applications. Furthermore, Kim and Lee, in 2021, formulated a probabilistic model for the non-suppression of electrical fires in fire brigades, using the MLE and relying on fire incident data from the Organization for Economic Cooperation and Development concerning the operation of nuclear power plants. This method was also applied to estimate the spatial variation coefficient (SVC) model using Gaussian processes as its basis (Dambon et al., 2020).

Previous investigations have also applied the MLE method in the field of earthquake. The method was used in likelihood analysis to evaluate the magnitude of the most significant seismic event, relying on certain statistical characteristics. Based on the analysis, while local characteristics might not be ideal for modeling the occurrence of seismic peaks, there was an observable correlation between some global properties and the largest magnitudes (Zaccagnino et al, 2023). Sharma and Biswas (2022) further showed that earthquake with a magnitude of 5,352 was considered the largest annual event in the Indo-Burmese region. It was also projected that large earthquake might likely occur over a wide period. On the other hand, Görgün (2013) reported that the distribution of low *b*-values for the series of Van–Erciş aftershocks in Turkey due to the cessation of the eastward mainshock rupture was considered a precursor phenomenon for future moderate to large magnitude earthquake. In 2017, Wang et al. used the MLE to fit non-local models while incorporating restricted local data, which included a case study assessing the likelihood of a significant earthquake occurring in Taipei. Therefore, this study aims to analyze seismicity level in multiple areas within Simeulue Regency and the adjacent regions in the Special Region of Aceh Province using the MLE method. The examination of seismicity level is closely linked to the determination of earthquake return period and the assessment of the risk level in these areas.

2. Data and Methods

The data used in this study consisted of earthquake records from period spanning 1940 to 2020 sourced online from the International Seismological Center (ISC) and the Indonesian Meteorology, Climatology, and Geophysical Agency (BMKG). These records included earthquake events with a magnitude equal to or greater than 3 on the Richter scale (SR) and a depth of 60 kilometers or less. The study area included Simeule Regency and its surroundings located at the coordinates 1°.97^'-3°.20' North Latitude and 95°.20^'-97°.05' East Longitude. Based on data from ISC and BMKG (from 1940-2020), 2,241 earthquake events have occurred in these areas.

Simeulue Regency consists of ± 40 large and small islands with 138 villages spread over 10 sub-districts, namely East Salang, Alafan, and Teluk Dalam. Simeulue Island is the largest in Regency and is located about 150 km from the coast to the west of Sumatra Island with an area of 2,051 km^2 (Syafwina, 2014). The Island together with other small ones is located in the west of Aceh Province.

In this study, the selected methodology was the traditional statistical method, specifically MLE. The distribution of earthquake epicenters was approximated using the GMT application, while the hypocenter was represented through a 3D scatterplot created using the MATLAB application. Moreover, seismic calculations were carried out using the Excel application. The foundational relationship between earthquake frequency and magnitude was initially introduced by Ishimoto & Iida in 1939, and subsequently extended by B. Guttenberg & C. F. Richter. This relationship was applied to both global seismic and specific regional datasets. The general formula commonly used stems from the empirical formula derived by B. Guttenberg & C. F. Richter, namely:

$$Log\ N(M) = a - bM \qquad (1)$$

where N(M) is the cumulative number of earthquake with a magnitude greater than or equal to M, M is the magnitude, *a* and *b* are seismic and tectonic parameters (Lin, 2010; Singh, 2014; & Han et al, 2015). Parameter *a* signifies the seismic activity of the area and is influenced by the fragility of the underlying rock, while *b* represents the slope or gradient of the linear equation depicting the relationship between earthquake frequency and magnitude. This slope characterizes the local stress activity and the greater the value of *a* in an area, the higher the seismic activity. Meanwhile, the value of *b* varies in each region depending on the rock structure that makes up the surface. Period and area of observation determine the level of seismicity. The values of *a* and *b* in Equation (1) were determined in this study using the MLE method.

The MLE method is a versatile statistical method, and one of its applications includes addressing seismological issues. This method was used to estimate the parameters of probability distributions by maximizing the likelihood function. Let $w_1, w_2, \dots, w_n$ be the value of a random sample from a population with parameter δ, the likelihood function (Kladivko and Rusy, 2022; Draper 1998; Walpole, 1982) of the sample would be

$$L(\delta) = g(w_1, w_2, \dots, w_n; \delta) = \prod_{i=1}^{n} g(w_i, \delta),$$

where $g(w_1, w_2, \dots, w_n; \delta)$ is the value of joint probability density or joint probability distribution of the random variables $W_1, W_2, \dots, W_n$ at $W_1 = w_1,\ W_2 = w_2, \dots, W_n = w_n$. The MLE method comprises the process of maximizing the likelihood function with respect to parameter δ. The maximum estimate of δ is the value at which the maximum likelihood function L(δ) reaches its peak during the relevant calculation. To find this value, the derivative of the logarithm of L(δ) was typically equated to zero, as represented by the equation:

$$\frac{\partial \log L(\delta)}{\partial \delta} = 0.$$

The Maximum Likelihood was used to analyze the relationship between earthquake frequency and magnitude (M). It is a statistical method often used to estimate the parameters of probability distributions and model this relationship, particularly in seismic studies. Suppose a probability distribution function of M (Nava et al, 2017) was defined as;

$$h(M, \lambda) = \lambda e^{-\lambda(M - M_0)},\ M \geq M_0 \qquad (2)$$

If there are *n* earthquake with a magnitude $M_1, M_2, \dots, M_n$, then according to the likelihood function of Equations (1) and (2),

$$P(\lambda) = \prod_{i=1}^{n} h(M_i, \lambda)$$

$$= h(M_1,\lambda).\,h(M_2,\lambda) \ldots h(M_n,\lambda)$$

$$= \lambda^n e^{-\lambda \sum_{i=1}^{n}(M_i - M_0)}, \tag{3}$$

where

$$\lambda = \frac{b}{\log_{10} e}, \tag{4}$$

The estimated maximum likelihood of *b* was obtained from the relationship between Equations (3) and (4) (Smith, 1981; Henderson et al, 1994; Hiramatsu et al, 2000; Sharma et al, 2013; & Arubi et al, 2022),

$$b = \frac{\log e}{\bar{M} - M_0}, \tag{5}$$

where

$$\bar{M} = \frac{\sum_{i=1}^{n} M_i}{n},$$

is the average magnitude of earthquake, M_0 is the minimum magnitude, and log e = 0.434. The corresponding value of *a* calculated from the cumulative frequency relationship for $M \geq M_0$ would be:

$$a = \log N(M \geq M_0) + \log(b \ln 10) + M_0 b$$

To quantify the deviation in the calculation of the 'b-value' using the Maximum Likelihood method, the estimated parameters 'a' and 'b' were compared. The values were then used to compute seismicity index of earthquake. Earthquake seismicity index was determined using Equation (5) [Chasanah et al, 2013, Wally et al, 2023].

$$N_i(M \geq M_0) = 10^{a_i - \log(b_i \ln 10) - \log \Delta T - b_i M_0},$$
$$i = 1,2,\ldots,n \tag{6}$$

where Δt is the observation time interval.

Seismicity index is a metric that quantifies the overall count of earthquake events observed over a specific period, with magnitudes surpassing a defined threshold. On the other hand, return period represents the interval between occurrences of earthquake with the same magnitude in a particular area. The value was determined using Equation (6). [Chasanah et al, 2013, Wally et al, 2022]:

$$\theta_i(M \geq M_0) = \frac{1}{N_i(M \geq M_0)}, \tag{7}$$

where $\theta_i(M \geq M_0)$ is the *i*-th return period for magnitude $M \geq M_0$. On the other hand, $N_i(M \geq M_0)$ is the *i*th seismicity index for $M \geq M_0$ with M_0 being the smallest earthquake magnitude.

3. Result and Discussion

1.1.Seismic Attributes in Simeulue Regency and Surroundings

The study area comprised Simeulue Region, spanning multiple locations with coordinates between 1°.97' - 3°.18' North Latitude and 95°.29' - 97°.05' East Longitude (Figure 1a). Using data sourced from the ISC (International Seismological Center) and BMKG online, the study spanned an approximately 80-year period from 1940 to 2020. During this time frame, 2241 earthquake events with magnitudes greater than or equal to 3 and depths less than 60 km were recorded (1b).

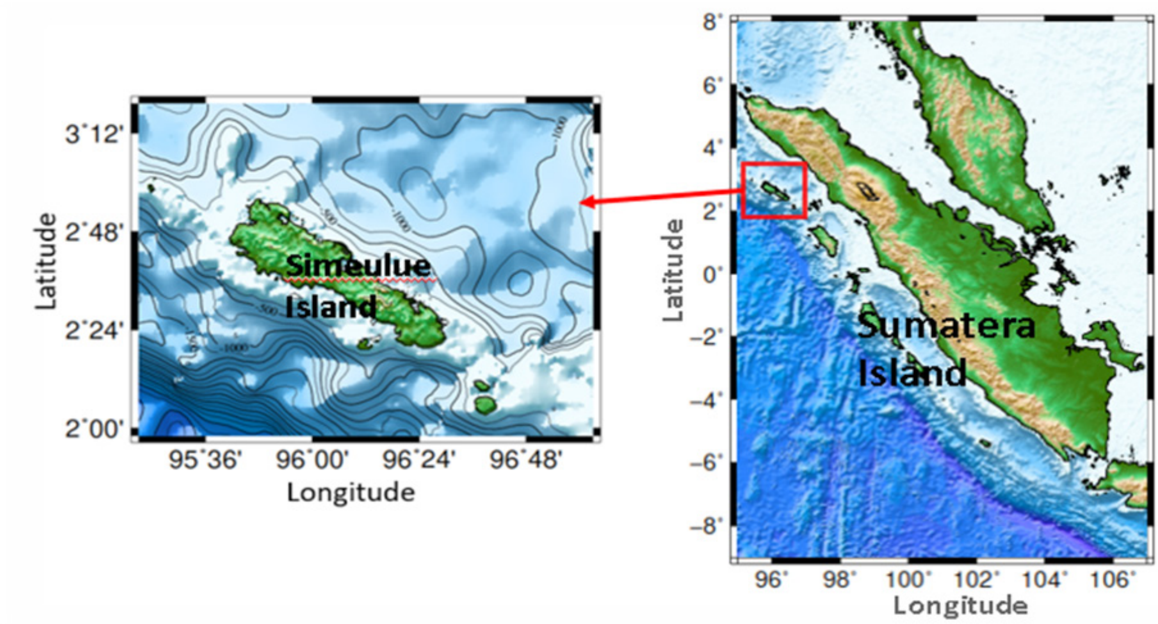

Figure 1. Study Area of Simeule Regency and Surroundings

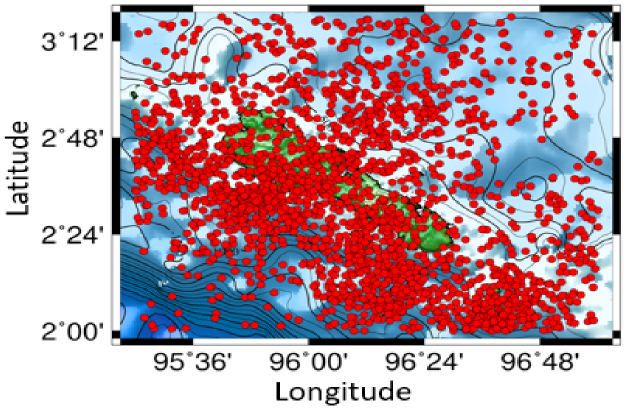

Figure 2. Spatial Distribution of Earthquake in the Study Region

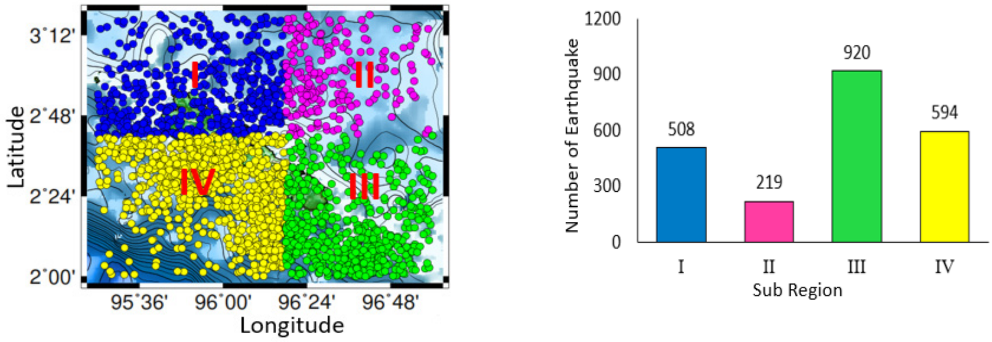

(a) (b)

Figure 2. (a) Map of Earthquake Distribution in Sub Regions, (b) Graph of Total Earthquake Distribution per Sub Region

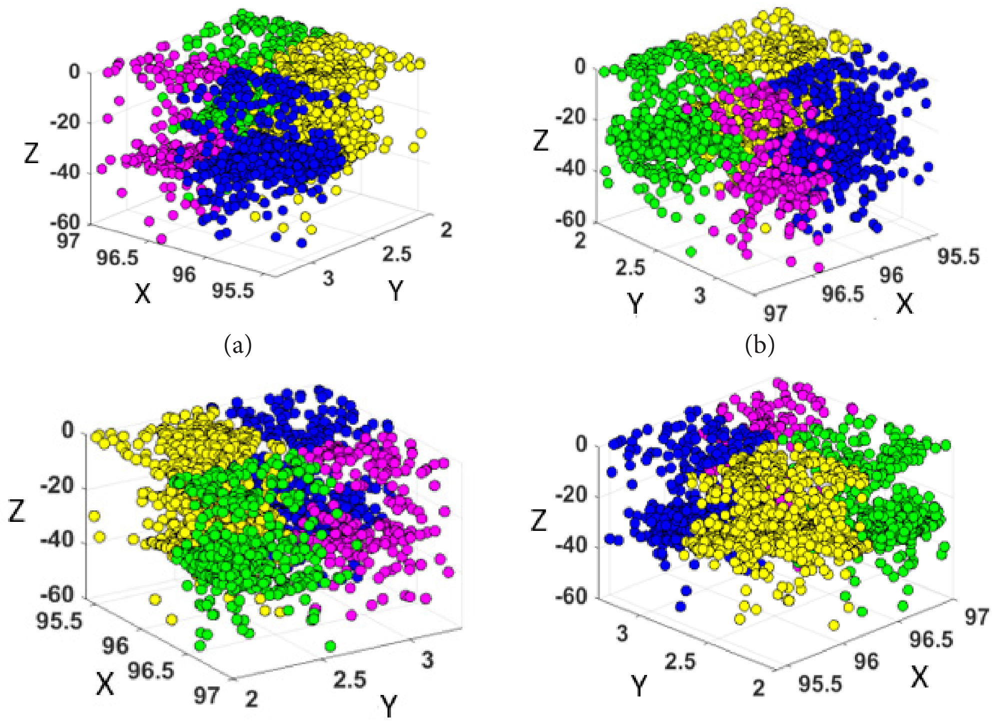

(a) (b)

(c) (d)

Figure 3. Earthquake distribution map based on depth in Sub Regions (a) I, b) II, (c) III, and d) IV

Based on Figure 1b, the distribution of earthquake in Simeule Regency and its surroundings was mostly in the sea area. Furthermore, the study area was divided into 4 Sub Regions (I, II, III, and IV). Sub-Region I was an area delineated by North Latitude coordinates ranging from 2°.42' to 3°.20' and East Longitude coordinates spanning from 95°.20' to 96°.18'. This region included the Alafan District, the western segment of Simeulue, sections of Salang, parts of the smaller Central Simeulue area, and approximately one-third of the Inner Bay. Sub Region II was part of the Indonesian Ocean with boundaries of a North Latitude: 2°.42' - 3°.20' and East Longitude: 96°.19' - 97°.05', while Sub Region III bounded by a North Latitude: 1°.56'

- 2°.42' and East Longitude: 96°.18' - 97°.05' included Sinabang City (Capital of Simeulue Regency), South Teupah, and a small part of East Simeulue District. On the other hand, Sub Region IV bounded by a North Latitude: 1°.97' - 2°.42' and East Longitude: 95°.24' - 96°.19' covered most of Central Simeulue District, mostly Teluk Dalam and West Teupah District. Sub-Region III, characterized by North Latitude coordinates ranging from 1°.56' to 2°.42' and East Longitude coordinates spanning from 96°.18' to 97°.05', comprised Sinabang City, the South Teupah, and a small section of the East Simeulue District. Additionally, Sub-Region IV, defined by North Latitude coordinates between 1°.97' and 2°.42' as well as East Longitude coordinates between 95°.24' and 96°.19', included a substantial portion of the Central Simeulue District, a major part of the Teluk Dalam, and a segment of the West Teupah District.

The distribution of earthquake in each region is shown in Figure 2a, with Sub Region III having the highest incidence (920), while the lowest (219) occurred in Sub Region II (Figure 2b).

The distribution of earthquake based on depth in Sub Regions I, II, III, and IV with a 3D scatterplot method is shown in Figure 3, with X = Longitude, Y= Latitude, and Z = Depth.

The distribution of earthquake depth was reviewed in 3 intervals (Figure 4a), namely 0-14.9 km, 15-44.9 km, and 45-59.9 km. Distribution based on magnitude grouping is shown graphically in Figure 4a. Based on the results, there was a dominance of earthquake in the 15 – 44.9 km (1643 events) depth interval compared to 0-14.9 km (549 events) while 549 events occurred at a depth interval of 45 - 59.9 km (Figure 4a). At depth intervals of 0-44.9 km and 15-44.9 km, Sub Region III had a larger number of occurrences while the smallest was recorded in Sub Region II. Furthermore, Sub Region I had the highest number at a depth interval of 45 – 59.9 km, and the least occurred in Sub Region III but was not significantly different from the other Sub Regions.

The magnitude distribution was divided into 4 groups, namely 3.0-3.9 Mw, 4.0 – 4.9 Mw, 5.0 – 5.9 Mw, and 6.0 – 6.9 Mw as shown graphically in Figure 4b. Based on the results, Sub Region III recorded more dominant events in the 3.0-3.9 Mw and 4.0-4.9 Mw intervals, while the least was in Sub Region II. Furthermore, Sub Region I had a higher frequency of earthquake events between the 5.0-5.9 Mw interval, and the least was recorded in Sub Region II. Sub Region I also showed a dominant occurrence in the interval magnitude of 6.0 – 6.9 Mw while no occurrence was reported in Sub Region III.

1.2. Seismic Activity Assessment in Simeulue Regency and Surroundings

The assessment of seismic activity level required several sequential steps. The initial phase entailed the computation of 'a-value' and 'b-value.' Subsequently, both values were determined for each of the Sub Regions (I, II, III, and IV) using the MLE method according to Equations (2) and (3). The computed results for 'a' and 'b' in each region are presented in Table 1.

Based on Table 1, the *a*-value of Sub Region III was greater compared to others, showing that this area had high seismic activity. The lowest value was recorded in Sub Region IV, meaning that this area had lower seismic activity compared to others (Figure 5).

Figure 6 shows the spatial variation of seismotectonic parameters for *a*-values in each Sub Region (Figure 6). The 'a-value' in Sub Region I ranged from 4.1 to 8.1, with the highest occurring in the Sembilan Village, West Simeulue District. In Sub Region II, the value ranged between 4 to 8.5, and the highest was found in the sea area. On the other hand, in Region III, the 'a-value' varied between 5 and 17.2, with the highest also reported in the sea area. In Sub Region IV, it ranged from 3.9 to 6.5, and the highest was found in the East Simeulue, South Teupah, and predominantly in the sea area.

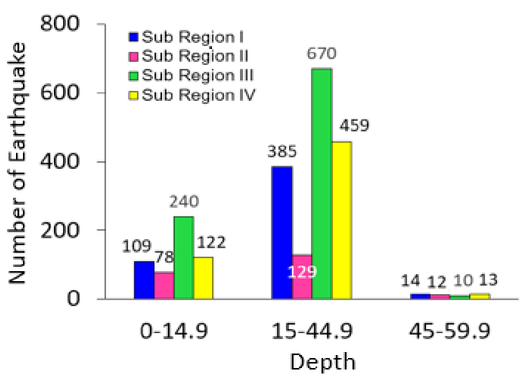

(a)

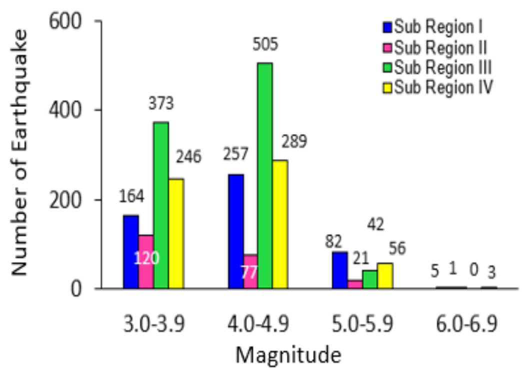

(b)

Figure 4. Number of Earthquake by a) Depth and b) Magnitude

Table 1. *a*-value and *b*-value for each Sub Region

Sub Region	*a*-value	*b*-value
I	3.297	0.376
II	3.478	0.498
III	4.389	0.630
IV	3.271	0.386

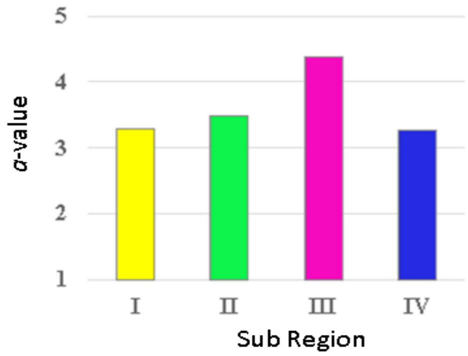

Figure 5. Spatial variation of *a*-value seismotectonic parameters in Sub Region a) I, b) II, c) III, and d) IV

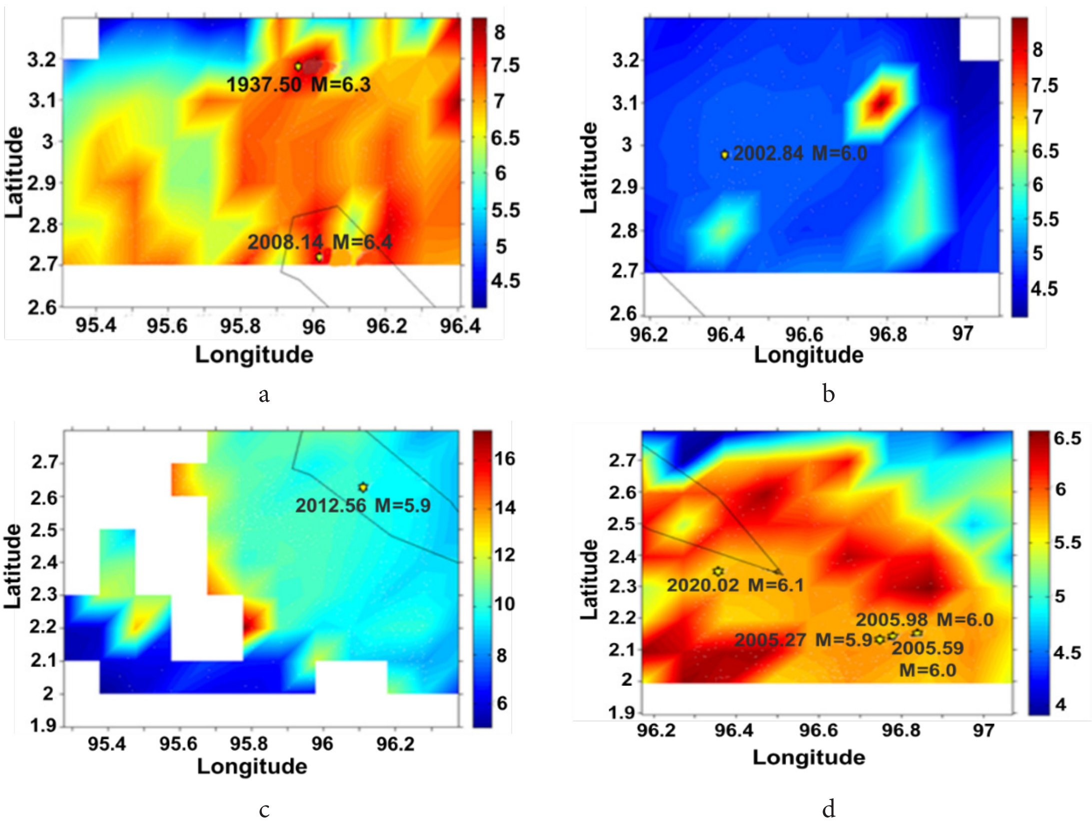

Figure 6. The Spatial variation of b-value seismotectonic parameters Sub Region a) I, b) II, c) III, and d) IV

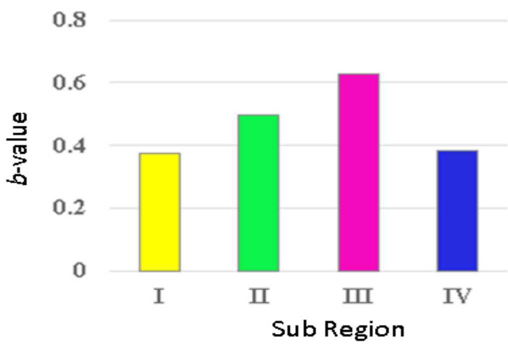

Figure 7. *b*-value for each Sub Region (I, II, III, and IV)

The *b*-value in Sub Region III was greater compared to others, suggesting that the rocks in this area could be classified as brittle rocks (heterogeneous), with relatively low-stress level due to their frequent release in the form of seismic waves (Table 1). The *b*-value in the four Sub Regions are graphically presented in Figure 7.

The spatial variation of *b*-value seismotectonic parameters for each Sub Region based on map color gradations is shown in Figure 8.

Based on Figure 8, the *b*-value in Sub Region I ranged from 0.59 to 1.38 with the highest occurring in the Sembilan Village, West Simeulue District, and predominantly in the

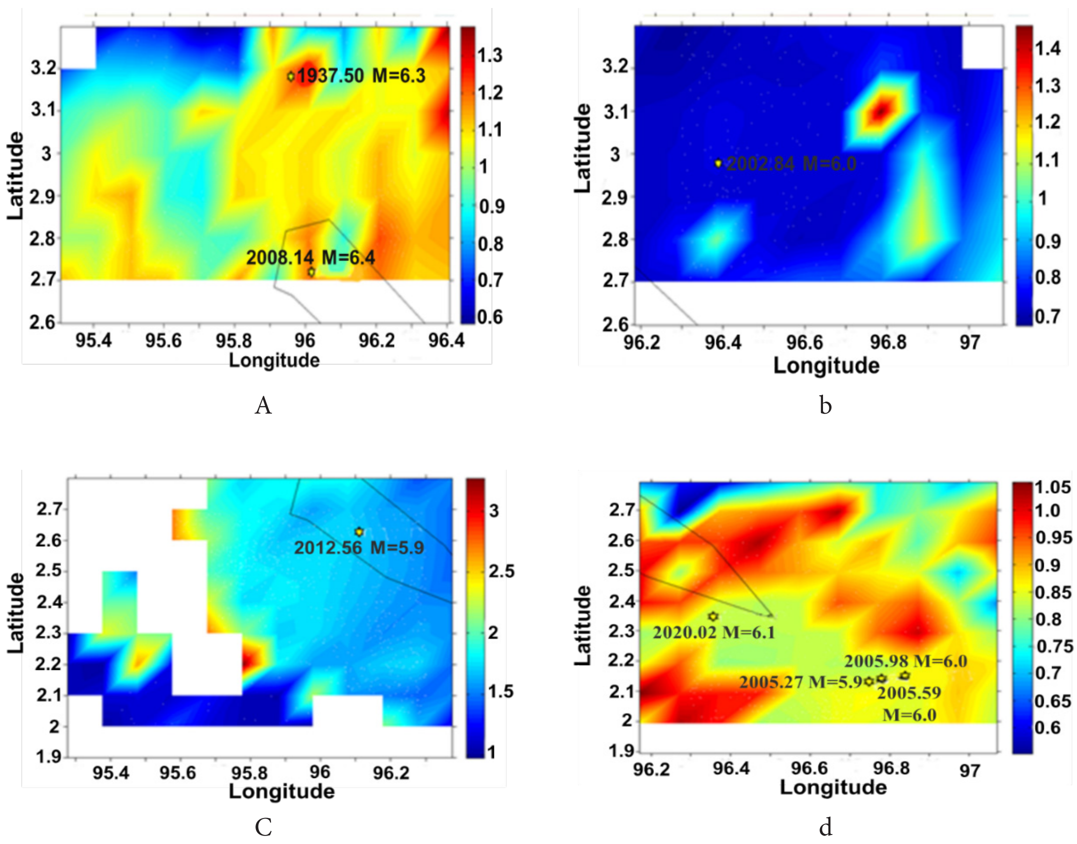

Figure 8. The spatial variation of *b*-value seismotectonic parameters for Sub Region a) I, b) II, c) III, and d) IV

Table 3. Relationship between Earthquake Frequency and Magnitude of Each Sub Region

Sub Region	$Log\ N(M) = a - bM$
I	$3{,}297 - 0{,}376M$
II	$3{,}478 - 0{,}498M$
III	$4{,}389 - 0{,}630M$
IV	$3{,}271 - 0{,}386M$

sea area. On the other hand, the value for Sub Region II was between 0.68 and 1.46 with the highest being reported in the sea area. In Sub Region III, the *b*-value ranged from 1 to 3.3 with the highest value being in the sea area. This value in Sub Region IV was between 0.55 and 1.05 with the highest being found at East Simeulue, South Teupah, and mostly in the sea area.

Based on the *a*-value and *b*-value obtained, the relationship between the frequency and magnitude of earthquake (Equation 1) for each Sub region was assessed (Table 3).

Based on Figure 9, the Mc value was 4.8 showing that the frequency of earthquake with a magnitude greater than 4.8 in Sub this area would decrease. This pattern also applied to Sub Regions II, III, and IV, namely earthquake with magnitudes greater than 3.9, 4.7, and 4.1 would decrease. The Mc value was obtained using the MLE method, and the red linear line in each region showed the GRL empirical equation (Table 3).

The subsequent stage comprised computing seismicity index and earthquake return period. Based on Equation (5), seismicity index was determined for Sub Regions I, II, III, and IV, with magnitude categories of $3.0 \leq M < 4.0, 4.0 \leq M < 5.0, 5.0 \leq M < 6.0$, and $M \geq 6.0$ (Table 4).

As shown in Table 4, for the magnitude range of $3.0 \leq M < 4.0$, Sub Region III showed the highest seismicity index at 2,719, and the lowest was observed in Sub Region II at 1,051. In the $4.0 \leq M < 5.0$ range, Sub Region I showed the highest seismicity index at 0.896, and Sub Region II had the lowest at 0.334. In the $5.0 \leq M < 6.0$ and $M \geq 6.0$ categories, Sub Region I had the highest seismicity index of 0.377 and 0.159, while the lowest index was found in Sub Region II at 0.106 and 0.034 respectively.

Based on Figure 10, the larger the magnitude value, the smaller seismicity index. Using Equation (6), earthquake return period for each Sub Region (I, II, III, and IV) with magnitude intervals ($3.0 \leq M < 4.0$, $4.0 \leq M < 5.0$, $5.0 \leq M < 6.0$, and $M \geq 6.0$) was calculated and the results are shown in Table 5.

Based on Table 5, for the magnitude $3.0 \leq M < 4.0$ $3.0 \leq M < 4.0$, the longest earthquake return period was found in Sub Region II at 0.952 years or 347 days, while the fastest was recorded in Sub Region III, at 0.368 years or 134

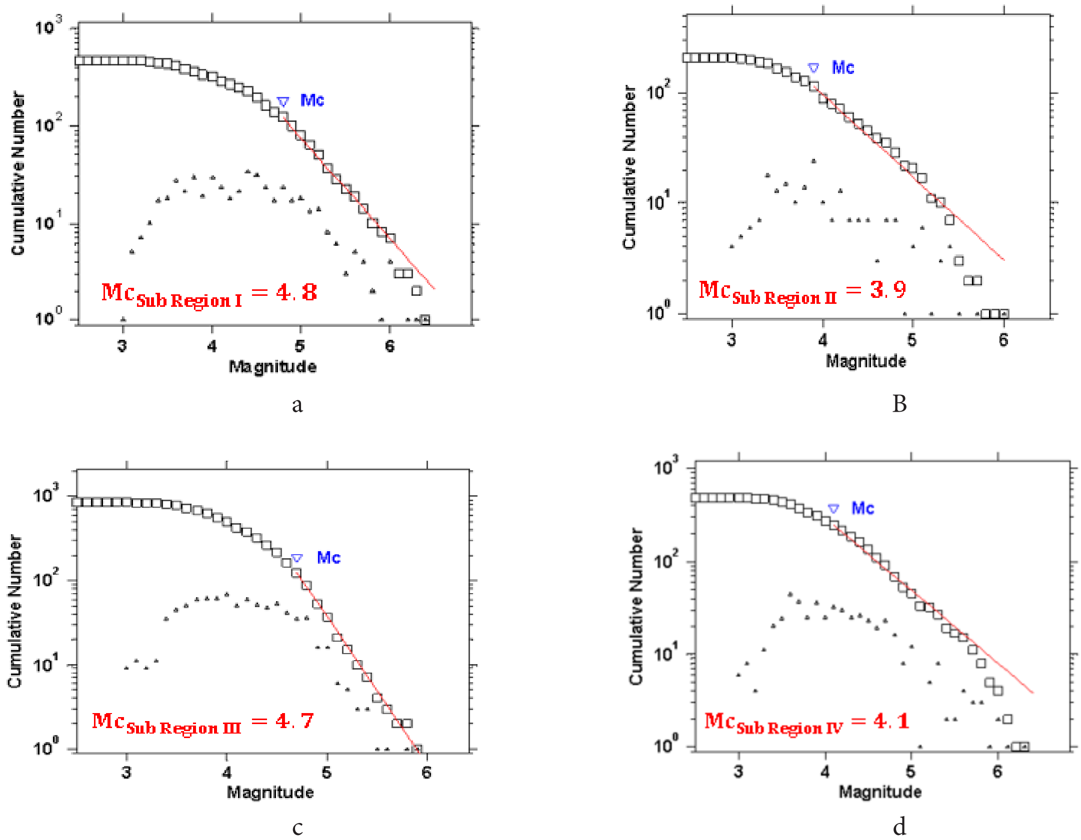

Figure 9. The spatial variation map of a-value Sub Regions a) I, b) II, c) III, and d) IV

Table 4. Results of seismicity index analysis

Sub Region	Seismicity Index			
	$3.0 \leq M < 4.0$	$4.0 \leq M < 5.0$	$5.0 \leq M < 6.0$	$M \geq 6{,}0$
I	2.131	0.896	0.377	0.159
II	1.051	0.334	0.106	0.034
III	2.719	0.637	0.149	0.035
IV	1.824	0.750	0.308	0.127

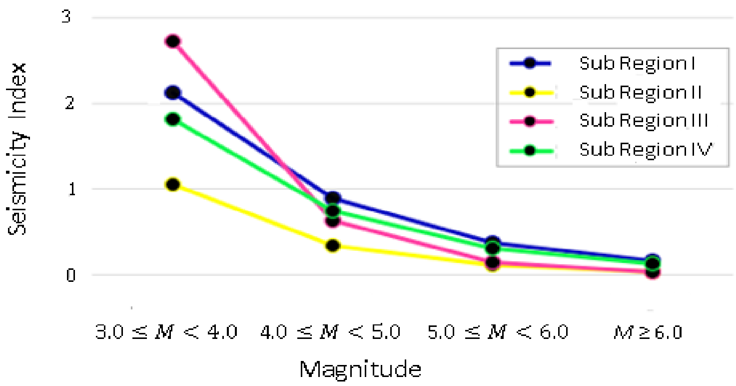

Figure 10. Relation Magnitude and Seismicity Index

days. In the $4.0 \leq M \leq 5.04.0 \leq M \leq 5.0$ magnitude, the longest earthquake return period was found in Sub Region II, estimated at 2,996 years or 1,094 days, while the fastest was in Sub Region I, at 1.116 years or 407 days.

For $5.0 \leq M < 6.05.0 \leq M < 6.0$, the longest earthquake return period was in Sub Region II, at 9.431 years or 3.442 days, while the fastest was recorded in Sub Region I, at 2.652 years or 968 days. In $M \geq 6.0$ magnitude, the longest period was in Sub Region II, at 29.685 years or 10.835 days, while the fastest was in Sub Region I, at 6.302 years or 2.300 days.

Based on Figure 11, the greater the magnitude, the longer return period. Therefore, it was concluded that earthquake with large magnitudes rarely occur due to the long return period.

Table 5. Results of earthquake Return Period Analysis

Sub Region	Repeat Period of Earthquakes			
	$3.0 \leq M < 4.0$	$4.0 \leq M < 5.0$	$5.0 \leq M < 6.0$	$M \geq 6,0$
I	0.469	1.116	2.652	6.302
II	0.952	2.996	9.431	29.685
III	0.368	1.569	6.693	28.553
IV	0.548	1.333	3.243	7.887

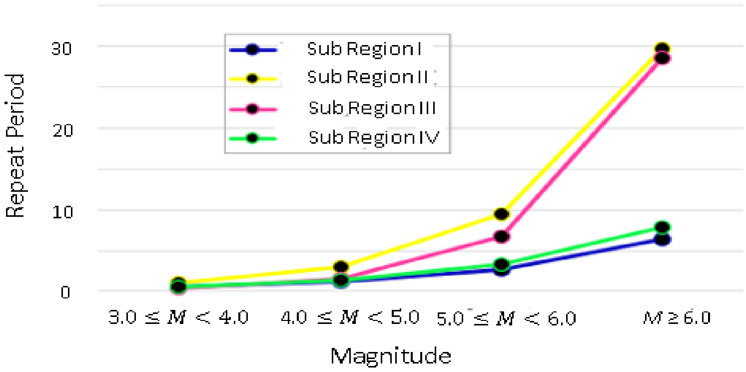

Figure 11. Relation Magnitude and Repeat Period

4. Conclusion

In conclusion, the results showed that the highest earthquake distribution in Simeulue Regency and its adjacent areas occurred in Sub Region III, with the majority (1,643 events) occurring at a depth between 15 and 44.9 km. This area also showed a more prominent distribution of events within the magnitude range of 3.0 to 4.9 Mw. Furthermore, Sub Region I had the highest Mc value of 4.8 compared to II, III, and IV, suggesting the occurrence of earthquake with a magnitude exceeding 4.8 would be less frequent. This trend was consistent across Mc values for the other Sub Regions including II, III, and IV. It was also found that Sub-Region III had the largest *a*-value and *b*-value as well as the highest seismicity index for magnitude M≥3.0. On the other hand, Sub-Region I had the highest seismicity index for each magnitude. Sub Region II was found to have longer periodic return for each magnitude interval ($3.0 \leq M < 4.0$, $4.0 \leq M < 5.0$, $5.0 \leq M < 6.0$, and $M \geq 6.0$). The results also showed that Sub Region III had the shortest return period for intervals of magnitude $3.0 \leq M < 4.0$, while Sub Region I showed the shortest return period for $4.0 \leq M < 5.0$, $5.0 \leq M < 6.0$, and $M \geq 6.0$.

Acknowledgement

The authors would like to thank the anonymous reviewers for commenting on earlier version of this paper.

References

S. Nampally, S. Padhy, & V.P. Dimri (2018). Characterizing spatial heterogeneity based on the b-value and fractal analyses of the 2015 Nepal earthquake sequence. Tectonophysiscs, vol. 722, pp. 154-162.

R. Lines, J.P.P., Walker, & R. Yore,(2022). Progression through emergency and temporary shelter, transitional housing and permanent housing: A longitudinal case study from the 2018 Lombok earthquake, Indonesia. International Journal of Disaster Risk Reduction, vol. 75, pp. 1-14.

M. A., Jafari, (2010). Statistical prediction of the next great earthquake around Tehran, Iran. Journal of Geodynamics, vol. 49, pp. 14-18..

F.A. Nava, L.A. Barrientos, V.H.M. Ramirez, I. Tores, & F.R. Zuniga (2027). Sampling uncertainties and source b likelihood for the Gutenberg-Richter b value from the Aki-Utsu method, Journal of Seismology. vol.22, no.3., pp. 1-10.

E. Luschen, C. Muller, H.Koop, M. Engels, R. Luts, L. Planert, A. Shulgin, Y.S. Djajadiharja(2011). Structure, evolution, and tectonic activity of the eastern Sunda forearc, Indonesia, from marine seismic investigations. Tectonophysics, vol. 508, pp. 6-21.

F. Ramdani, P. Setiani, D.A. Setiawati(2019). Analysis of sequence earthquake of Lombok Island, Indonesia, Progress in Disaster Science. vol. 4, pp. 1-9.

A. J. Meltzner, K. Sieh, H-W. Chiang, C-C. Wu, L.L.H. Tsang, C-C. Shen, E.M. Hill, B.W. Suwargadi, D. H. Natawidjaja B. Philibosian, & R.W. Briggs(2015). Time-varying interseismic strain rates and similar seismic ruptures on the Niase Simeulue patch of the Sunda megathrust. Quaternary Science Reviews, vol. 122, pp. 258 – 281.

D. Zaccagnino, L. Telesca, & C. Doglioni (2023). Global versus local clustering of seismicity: Implications with earthquake prediction.Chaos, Solitons, and Fractals, vol. 170, no. 113419, pp. 1-8.

J. Henderson, I.G. Main, R.G. Pearce, & M. Takeya. (1994). Seismicity in north-eastern Brazil:fractal clustering and the evolution of the b-value. Geophysical Journal International, vol. 116, pp. 217-226.

M. Ishimoto, & K. Iida, (1939). Observation of earthquakes registered with the micro seismograph constructed recently. Bulletin of the Earthquake Research Institute. Vol. 17, pp. 443-478.

S. Sharma, S. Baruah, O.P. Sahu, P.K. Bora, & R. Duarah(2013). Low b-value prior to the Indo-Myanmar subduction zone earthquakes and precursory swarma before the May 1995 M 6.3 earthquake. Journal of Asia Earth Sciences. Vol. 73, pp. 176-183.

W.D. Smith(1981).The b-value as an earthquake precursor. Nature. Vol. 289, pp. 136-139.

Syafwina(2014).Recognizing indigenous knowledge for disaster management: Smong, Early warning system from Simeulue Island, Aceh", The 4th International Conference on Sustainable Future for Human Security. SustaiN 2013. Procedia Environmental Sciences. Vol 20.

Y. Hiramatsu, N. Hayashi, & M. Furumoto(2000). Temporal changes in coda Q^{-1} and b value due to the static stress change associated with the 1995 Hyogo-ken Nanbu earthquake. Journal of Geophysical Research. vol 105, No. B3, pp. 6141-6151.

D. Arubi, Zulfakriza, S. Rosalia, D.P.Sahara, & N.T. Puspito(2022). Estimation of B-Value Variation as Earthquake Precursor in Java Region with Maximum Likelihood Method. 1st International Seminar on Earth Sciences and Technology 2022, IOP Conf. Series: Earth and Environmental Science. Vol 1047.

U. Chasanah, Madlazim, & T. Prastowo(2013). Analisis tingkat seismisitas dan periode ulang gempa di Sumatera Barat pada Periode 1961-2010. Jurnal Fisika, vol.02, no. 02, pp. 1-5.

I. Wally, H.J. Wattimanela, & Y.A. Lesnussa. Analysis of earthquake activity level in several districs in the Province of Aceh with using the Gutenberg-Richter Method approach", The 7th International Conference on Basic Sciences 2021 (ICBS 2021). AIP Conference Proceedings. Vol. 588.

I.F.A. El-Nader, A. Shater, & H.M. Hussein(2016). Mapping b-values beneath Abu Dabbab from June to August 2004 earthquake swarma. NRIAG Journal of Astronomy and Geophysics. Vol. 5, pp. 403-412.

S. Gunti, P. Roy, J. Narendran, R. Pudi, S. Muralikrishnan, K.V. Kumar, M. Subrahmanyam, Y. Israel, & B.S. Kumra, (2022). Assessment of geodetic strain and stress variations in Nepal due to 25 April 2015 Gorkha earthquake: Insights from the GNSS data analysis and b-value. Geodesy and Geodynamics. Vol. 13, pp. 288-300.

V.Sharma, & R. Biswas (2022). Probabilistic earthquake hazard parameterization for Indo-Burma region using extreme value approach. Natural Hazards Research. Vol. 2., no. 279286, pp. 279-286.

E. Gorgun (2013). Analysis of the b-values before and after the 23 October 2011 Mw 7.2 Van-Ercis, Turkey earthquake. Tectonophysics, vol 99, pp. 213-221.

J.P. Wang, Yun Xu, & Yih-Min Wu (2017). Earthquake probability in Taipei based on non-local model with limited local observation: Maximum likelihood estimation. Soil Dynamics and Earthquake Engineering. Vol. 99, pp. 150-156.

A. Rahman, A. Sakurai, & K. Munadi (2018).The analysis of the development of the Smong story on the 1907 and 2004 Indian Ocean tsunamis in strengthening the Simeulue island community's resilience. Vol. 29, pp. 13-23, 1 August 2018.

C. Singh(2014). Spatial variation of seismic b-value across the NW Himalaya. Geomatics, Natural Hazards, and Risk. Vol. 7, no.2, pp. 522-530.

Q. Han, L. Wang, J. Xu, A. Carpinteri, & G. Lacidogna (2015). A robust method to estimated the b-value of the magnitude-frequency distribution of earthquakes. Chaos, Solitons, and Fractals, vol. 81, pp. 103-110.

C-H. Lin (2010). Temporal b-value variations throughout a seismic faulting process: The 2008 Taoyuan Earthquake in Taiwan. Terr. Atmos. Ocean.Sci. Vol.21, no.2, pp.229-234.

R.E. Walpole (1982). *Introduction to Statistics*, 3rd Edition, Macmillan Publishing Company, Inc., New York.

N. R. Draper, & H. Smith (1998). *Applied Regression Analysis*, Third Edition, John Wiley & Sons. Inc, New York.

K. Kladivko & T. Rusy (2022). Maximum Likelihood Estimation of the Hull-White model, Journal of Empirical Finance, vol 70, pp 227-247.

F. Liu (2022). A comparison between multivariate linear model and maximum likelihood estimation for the prediction of elemental composition of coal using proximate analysis, Results in Engineering, vol 13.

S. Kim & S. Lee (2021). Maximum likelihood estimation of probabilistic non-suppression model for OECD NPP electrical fire applying non-negative continuous distribution, Fire Safety Journal, vol 122, pp. 1-7.

J.A. Dambon, F. Sigrist, & R. Furrer (2020). Maximum likelihood estimation of spatially varying coefficient models for large data with an application to real estate price prediction, Spatial Statistics, vol 41, pp. 1-21.